Grey Matter Atrophy and its Relationship with White Matter Lesions in Patients with Myelin Oligodendrocyte Glycoprotein Antibody-associated Disease, Aquaporin-4 Antibody-Positive Neuromyelitis Optica Spectrum Disorder, and Multiple Sclerosis

Rosa Cortese, MD, PhD [1,2] Marco Battaglini, PhD,[1,3] Ferran Prados, PhD,[2,4,5]
Giordano Gentile, PhD,[1,3] Ludovico Luchetti, BASc,[1,3] Alessia Bianchi, MD, PhD [2]
Lukas Haider, MD, PhD [2] Anu Jacob, MD, PhD,[6,7] Jacqueline Palace, MD, PhD,[8]
Silvia Messina, MD, PhD [8] Friedemann Paul, MD [9] Romain Marignier, MD, PhD [10]
Françoise Durand-Dubief, MD,[10] Carolina de Medeiros Rimkus, MD,[11]
Samira Luisa Apostolos Pereira, MD,[12] Douglas Kazutoshi Sato, MD, PhD [13]
Massimo Filippi, MD, PhD [14,15,16,17,18] Maria Assunta Rocca, MD, PhD [14,15,18]
Laura Cacciaguerra, MD, PhD,[14,15] Àlex Rovira, MD [19]
Jaume Sastre-Garriga, MD, PhD [20] Georgina Arrambide, MD, PhD,[20]
Yaou Liu, MD, PhD [21] Yunyun Duan, MD,[21] Claudio Gasperini, MD, PhD [22]
Carla Tortorella, MD, PhD,[22] Serena Ruggieri, MD, PhD,[23,24]
Maria Pia Amato, MD, PhD,[25,26] Monica Ulivelli, MD,[1] Sergiu Groppa, MD, PhD,[27]
Matthias Grothe, MD [28] Sara Llufriu, MD, PhD [29] Maria Sepulveda, MD,[29]
Carsten Lukas, MD, PhD [30,31] Barbara Bellenberg, PhD,[30] Ruth Schneider, MD,[30,31]
Piotr Sowa, MD, PhD,[32] Elisabeth G. Celius, MD, PhD,[33]
Anne-Katrin Pröbstel, MD, PhD [34] Cristina Granziera, MD, PhD,[34,35] Özgür Yaldizli, MD,[34]
Jannis Müller, MD [34,35] Bruno Stankoff, MD, PhD [36] Benedetta Bodini, MD, PhD,[36]
Frederik Barkhof, MD, PhD,[4,37] Olga Ciccarelli, MD, PhD,[2,38†]
Nicola De Stefano, MD, PhD,[1†] for the MAGNIMS Study Group

Objective: To evaluate: (1) the distribution of gray matter (GM) atrophy in myelin oligodendrocyte glycoprotein antibody-associated disease (MOGAD), aquaporin-4 antibody-positive neuromyelitis optica spectrum disorder (AQP4 +NMOSD), and relapsing–remitting multiple sclerosis (RRMS); and (2) the relationship between GM volumes and white

matter lesions in various brain regions within each disease.

Methods: A retrospective, multicenter analysis of magnetic resonance imaging data included patients with MOGAD/ AQP4+NMOSD/RRMS in non-acute disease stage. Voxel-wise analyses and general linear models were used to evaluate the relevance of regional GM atrophy. For significant results ($p < 0.05$), volumes of atrophic areas are reported.

Results: We studied 135 MOGAD patients, 135 AQP4+NMOSD, 175 RRMS, and 144 healthy controls (HC). Compared with HC, MOGAD showed lower GM volumes in the temporal lobes, deep GM, insula, and cingulate cortex (75.79 cm^3); AQP4+NMOSD in the occipital cortex (32.83 cm^3); and RRMS diffusely in the GM (260.61 cm^3). MOGAD showed more pronounced temporal cortex atrophy than RRMS (6.71 cm^3), whereas AQP4+NMOSD displayed greater occipital cortex atrophy than RRMS (19.82 cm^3). RRMS demonstrated more pronounced deep GM atrophy in comparison with MOGAD (27.90 cm^3) and AQP4+NMOSD (47.04 cm^3). In MOGAD, higher periventricular and cortical/juxtacortical lesions were linked to reduced temporal cortex, deep GM, and insula volumes. In RRMS, the diffuse GM atrophy was associated with lesions in all locations. AQP4+NMOSD showed no lesion/GM volume correlation.

Interpretation: GM atrophy is more widespread in RRMS compared with the other two conditions. MOGAD primarily affects the temporal cortex, whereas AQP4+NMOSD mainly involves the occipital cortex. In MOGAD and RRMS, lesion-related tract degeneration is associated with atrophy, but this link is absent in AQP4+NMOSD.

Myelin-oligodendrocyte glycoprotein antibody-associated disease (MOGAD), aquaporin-4 antibody-positive neuromyelitis optica spectrum disorder (AQP4+NMOSD), and multiple sclerosis (MS), are the most common demyelinating disorders of the central nervous system (CNS), whose differential pathogenetic mechanisms are still being investigated.[1] While MS can show relapses and a progressive course, MOGAD and AQP4+NMOSD are currently regarded as purely relapsing diseases without clinical progression.[2,3] Although MOGAD, AQP4+NMOSD, and MS can share similar clinical and imaging characteristics, additional radiological features that can differentiate these three diseases in clinical practice have been identified.[4,5]

These distinctive clinical and imaging features suggest that the underlying mechanisms of damage and repair differ significantly among the three diseases. In MS, neuropathological data consistently reveal the coexistence of focal inflammatory demyelination and neurodegenerative processes, which are closely interconnected.[6] AQP4+NMOSD is characterized by extensive destruction of astrocytes, with

Address correspondence to Dr Rosa Cortese, Department of Medicine, Surgery and Neuroscience, University of Siena, Siena, Italy.
E-mail: rosa.cortese@unisi.it

†Joint last authors.

From the [1]Department of Medicine, Surgery and Neuroscience, University of Siena, Siena, Italy; [2]Queen Square MS Center, Department of Neuroinflammation, UCL Queen Square Institute of Neurology, Faculty of Brain Sciences, University College London, London, UK; [3]SIENA imaging SRL, Siena, Italy; [4]Center for Medical Imaging Computing, Medical Physics, and Biomedical Engineering, UCL, London, UK; [5]E-Health Center University Oberta de Catalunya, Barcelona, Spain; [6]NMO Clinical Service at the Walton Centre, Liverpool, UK; [7]Department of Neurology, Cleveland Clinic, Abu Dhabi, UAE; [8]Department of Clinical Neurology, John Radcliffe Hospital, Oxford, UK; [9]Experimental and Clinical Research Center, Max Delbrueck Center for Molecular Medicine and Charité-Universitaetsmedizin Berlin, Berlin, Germany; [10]Department of Neurology, Multiple Sclerosis, Myelin Disorders, and Neuro-inflammation, Pierre Wertheimer Neurological Hospital, Hospices Civils de Lyon, Lyon, France; [11]Department of Radiology and Oncology, Faculty of Medicine, University of São Paulo (FMUSP), São Paulo, Brazil; [12]Department of Neurology, Faculty of Medicine, University of São Paulo (FMUSP), São Paulo, Brazil; [13]Pontifical Catholic University of Rio Grande do Sul (PUCRS), School of Medicine, Porto Alegre, Brazil; [14]Neuroimaging Research Unit, Division of Neuroscience, IRCCS San Raffaele Scientific Institute, Milan, Italy; [15]Neurology Unit, IRCCS San Raffaele Scientific Institute, Milan, Italy; [16]Neurorehabilitation Unit, IRCCS San Raffaele Scientific Institute, Milan, Italy; [17]Neurophysiology Service, IRCCS San Raffaele Scientific Institute, Milan, Italy; [18]Vita-Salute San Raffaele University, Milan, Italy; [19]Section of Neuroradiology, Department of Radiology, Hospital Universitari Vall d'Hebron, Universitat Autònoma de Barcelona, Barcelona, Spain; [20]Multiple Sclerosis Centre of Catalonia (Cemcat), Department of Neurology, Hospital Universitari Vall d'Hebron, Universitat Autònoma de Barcelona, Barcelona, Spain; [21]Department of Radiology, Beijing Tiantan Hospital, Capital Medical University, Beijing, China; [22]Department of Neurosciences, S. Camillo-Forlanini Hospital, Rome, Italy; [23]Department of Human Neurosciences, Sapienza University of Rome, Rome, Italy; [24]Neuroimmunology Unit, IRCSS Fondazione Santa Lucia, Rome, Italy; [25]Department Neurofarba, University of Florence, Florence, Italy; [26]IRCCS Don Carlo Gnocchi Foundation, Florence, Italy; [27]Department of Neurology, University Medical Center of the Johannes Gutenberg University Mainz, Mainz, Germany; [28]Department of Neurology, University Medicine of Greifswald, Greifswald, Germany; [29]Service of Neurology, Laboratory of Advanced Imaging in Neuroimmunological Diseases, Center of Neuroimmunology, Hospital Clínic of Barcelona, Institut d'Investigacions Biomèdiques August Pi i Sunyer (IDIBAPS), and Universitat de Barcelona, Barcelona, Spain; [30]Institute of Neuroradiology, St. Josef Hospital, Ruhr University Bochum, Bochum, Germany; [31]Department of Neurology, St. Josef Hospital, Ruhr University Bochum, Bochum, Germany; [32]Division of Radiology and Nuclear Medicine, Oslo University Hospital, Oslo, Norway; [33]Department of Neurology, Oslo University Hospital and Faculty of Medicine, University of Oslo, Oslo, Norway; [34]Department of Neurology, Biomedicine and Clinical Research, and Research Center for Clinical Neuroimmunology and Neuroscience Basel, University Hospital and University of Basel, Basel, Switzerland; [35]Translational Imaging in Neurology (ThINk) Basel, Department of Biomedical Engineering, University Hospital Basel and University of Basel, Basel, Switzerland; [36]Sorbonne University, Paris Brain Institute, ICM, Pitié Salpêtrière Hospital, Paris, France; [37]Radiology & Nuclear medicine, VU University Medical Center, Amsterdam, The Netherlands; and [38]National Institute for Health Research (NIHR) University College London Hospitals (UCLH) Biomedical Research Center, London, UK

Additional supporting information can be found in the online version of this article.

secondary demyelination.[7] Conversely, in MOGAD, neuropathological studies are limited and reported different features, including extensive demyelination with relatively preserved axons, and reactive gliosis in both white (WM) and GM.[8]

Magnetic resonance imaging (MRI) is widely recognized as a reliable tool for studying in vivo brain pathological changes in the three diseases. Previous studies have primarily focused on WM lesions to differentiate between these diseases.[9–11] Alongside WM lesions, evaluating MRI-derived regional brain atrophy can offer important insights into their pathophysiology. Recent cross-sectional studies have demonstrated that brain atrophy, reflecting diffuse tissue damage and neurodegeneration, is present in all three diseases, albeit with varying patterns and degrees. Brain atrophy is more extensive in MS, whereas it is localized to specific regions of the GM in MOGAD and AQP4+NMOSD. However, data regarding GM involvement in the two antibody-mediated diseases are limited and conflicting.[11–14]

Previous MRI studies showed that there is a connection between focal brain lesions and GM atrophy in MS. These findings support the idea that WM damage may contribute to the accumulation of damage in the GM from the early stages of the disease.[15–18] Recent studies have proposed a similar effect of lesions on GM atrophy in MOGAD and AQP4+NMOSD, but the available data are limited and the results are controversial, possibly due to small sample sizes.[11–14] Understanding the interplay between focal inflammation, demyelination, and neurodegeneration in these three neurological disorders can enhance our understanding of how tissue damage accumulates and help differentiate their underlying mechanisms.

Given the existing knowledge gaps, we undertook a comprehensive study involving a multicenter cohort of individuals with MOGAD, AQP4+NMOSD, and MS. We used a voxel-based morphometry approach to: (1) identify and characterize patterns of GM atrophy specific to each of the three disorders, and (2) examine the relationship between GM volumes and the number of WM lesions in several brain locations within each disease.

Methods

Study Design and Population

This is a multicenter, retrospective study, conducted on data from 16 European and non- European centers that were collected as part of a Magnetic Resonance Imaging in Multiple Sclerosis (MAGNIMS) Collaboration (www.magnims.eu) project. From the original MAGNIMS cohort,[19] including 162 MOGAD, 162 AQP4+NMOSD, 189 MS, and 152 healthy controls (HC), we selected those with the following inclusion criteria: (1) diagnosis of MOGAD (which was made, in each center, only when MOGAD was suspected on the basis of patient's history and clinical presentation, and confirmed by MOG antibody positivity according to local laboratory guidelines), AQP4+NMOSD[20] or RRMS[21]; (2) serum antibodies detected using cell-based assay; (3) age at MRI ≥18 years; (4) being at least 6 months after an acute event; (5) having at least one sequence for WM lesion detection (either fluid-attenuated inversion recovery [FLAIR] or proton density/T2) and a 3D T1-weighted sequence with adequate quality (Fig S1).

Each participant provided written consent for research within each center. The final protocol for the analysis of fully anonymized scans, acquired independently at each center, was approved by the European MAGNIMS collaboration and by local ethics committees.

MRI Acquisition and Processing

MRI protocols and acquisition parameters of the centers were previously described.[19] MRI was acquired using a 3-T scanner for the majority of patients (87% MOGAD, 92% AQP4+NMOSD, 87% RRMS) and all HC. To assess lesion distribution, WM lesions were semi-automatically segmented on FLAIR/T2-sequences using a lesion prediction algorithm, as implemented in the LST toolbox version for SPM,[22] and lesion masks were created. Lesions were automatically classified, and defined as cortical/juxtacortical, periventricular, mixed deep GM/deep WM, deep WM, and infratentorial. Accuracy of classification was double-checked in each participant by two expert users according to previously published criteria[23] and manually edited when necessary. Ventricles, cortex, deep GM, and infratentorial masks were created using an in-house developed pipeline, using FSL tools (https:fsl.fmrib.ox.ac.uk). To investigate voxel-wise differences in GM volumes, we first created a study-specific GM mask template. This was performed by registering each participant-specific GM mask to a standard-specific space, which was then registered on the GM template previously created (Fig 1A, B).

Statistical Analysis

Means, medians, proportions of demographics, clinical features, and lesion characteristics were calculated for patients (and their subgroups) and HC. Differences were evaluated using Kruskal–Wallis, ANOVA, or χ^2-test, as appropriate.

The voxel-wise analyses were carried out using the GM masks as input images for the "randomize" tool (ie, the dependent variable). Within these masks, the "randomize" tool detects regions where GM volumes differ
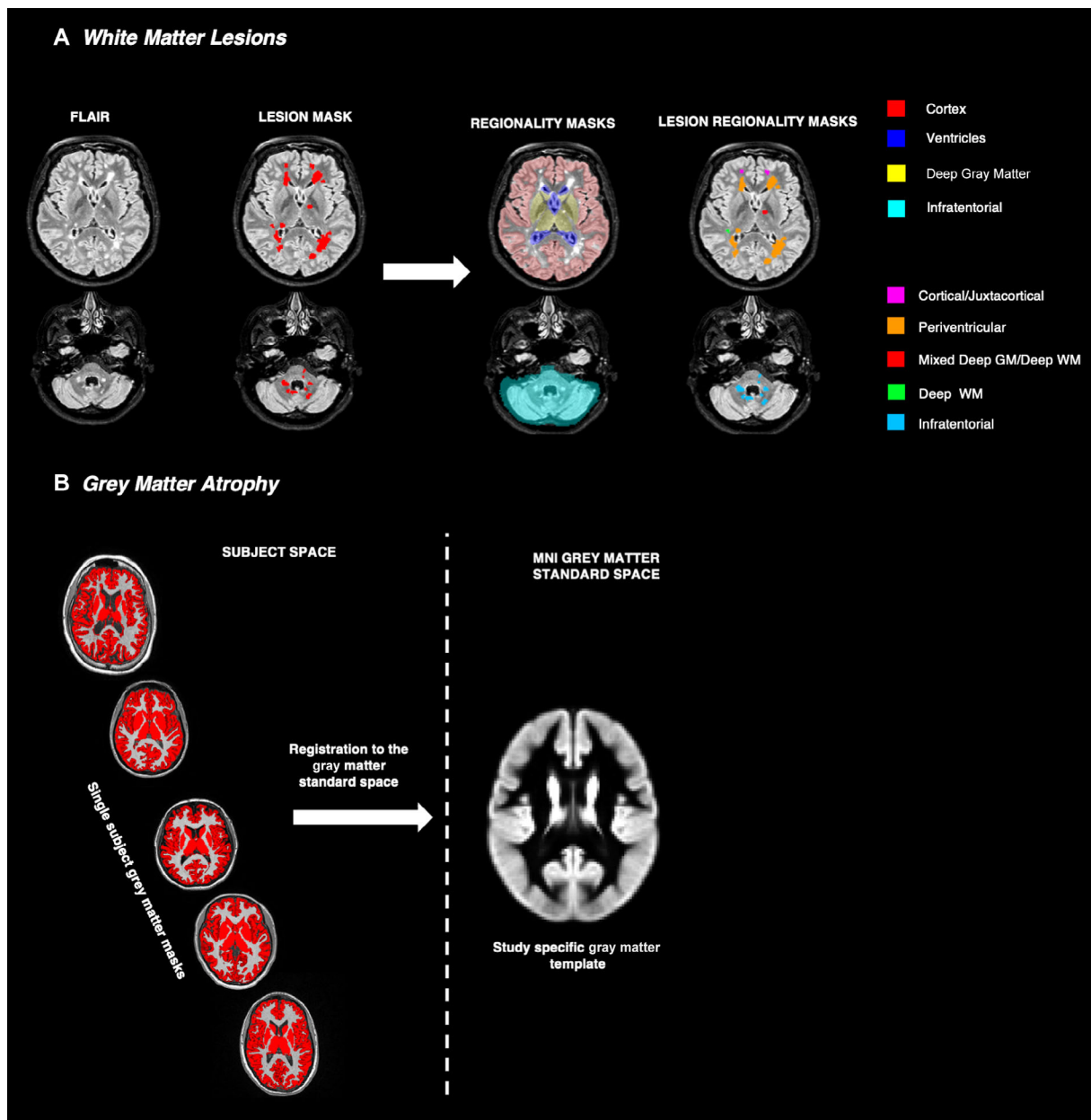
Figure 1: Image processing pipeline. The figure illustrates the processing steps to assess lesion distribution and voxel-wise atrophy analysis. (A) Lesions were semi-automatically segmented using a lesion segmentation tool, and then automatically classified as: cortical/juxtacortical, periventricular, mixed deep gray matter (GM)/deep white matter (WM), deep WM, or infratentorial, using previously created regionality maps. Lesion classification was double-checked accordingly to previously published criteria.[23] (B) To allow voxel-wise analyses of atrophy across participants, GM masks obtained by the SIENAX2 (Luchetti et al., ECTRIMS 2019) were non-linearly registered to the MNI 152 standard space using non-linear registration.[50] The resulting images were averaged and flipped along the x-axis to create a left–right symmetric, study-specific GM template. Then, all native GM images were non-linearly registered to this study-specific template and "modulated" to correct for local expansion (or contraction) due to the non-linear component of the spatial transformation. The modulated GM images were then smoothed with an isotropic Gaussian kernel with a sigma of 2 mm. This last step created the GM masks that were submitted into the voxel-wise statistical analysis to detect voxels with significant GM regional volume reduction. FLAIR = fluid-attenuated inversion recovery. [Color figure can be viewed at www.annalsofneurology.org]

between groups and where they correlate with lesion load.[24] This method uses nonparametric techniques, including label permutation and threshold-free cluster enhancement, to identify meaningful voxels by assessing label randomness and determining significant voxel clusters without predefining neighborhood size; thus, addressing multiple comparisons without relying on parametric approaches. Differences in GM volumes between groups were assessed using design matrices within general linear models, with disease as the variable of interest, and age, sex, disease duration and time to last attack, and centers as covariates, as appropriate. To assess the relationship

between lesions and GM atrophy in each patient group, a second design was used: first the number of lesions in each location was implemented as a regressor, while keeping age, sex and centers as covariates. Then, to assess partial correlation between different lesion locations, we focused on those areas that showed a significant correlation with atrophy in the previous analysis, and alternately used one location as regressor and implemented the others as covariates. Finally, we repeated the analysis using total T2-lesion volume as a regressor. Within each group, the anatomical location where brain atrophy significantly correlated with lesion activity was determined using predefined standard space masks (https://www.fmrib.ox.ac.uk/fsl/), as provided by the MNI structural atlas. For significant results ($p < 0.05$, corrected for multiple comparisons), the location of GM areas, the volume in cm^3, and the corresponding number of voxels resulting significantly different between patients' groups are reported. As some MOGAD and AQP4+NMOSD patients showed no brain lesions on MRI, all analyses were repeated considering patients separately with WM lesions and those without. Finally, differences in GM atrophy between AQP4+NMOSD and MOGAD were assessed in patients with a history of optic neuritis only (ON), with transverse myelitis only (TM) and with a history of both optic neuritis and transverse myelitis (ON + TM), until the date of the MRI scan.

Results

Study Population

We studied 135 MOGAD, 135 AQP4+NMOSD, 175 RRMS patients, and 144 HC. The demographic and clinical features of patients and HC are summarized in Table 1. Brain WM lesions were detected in 92/135 (68%) MOGAD, 108/135 (80%) AQP4+NMOSD, and all RRMS (100%) patients. Non-specific WM lesions were found in 33/144 (23%) of HC. The mean lesion number and volume were higher in RRMS than in both MOGAD and AQP4+NMOSD, with no differences between the two antibody-mediated diseases (Table 2).

Differences in GM Volumes Between Each Disease and Healthy Controls

When compared with HC, the three patients groups showed different patterns of GM atrophy. In particular, when considering the whole group (ie, patients with and without lesions), MOGAD showed atrophy in the temporal cortex, deep GM, insula, cingulate cortex, and cerebellum (total volume of atrophic voxels 75.79 cm^3). Patients with AQP4+NMOSD showed atrophy in the occipital cortex (32.83 cm^3). In RRMS, atrophy was widespread within the cortex, deep GM, and cerebellum (total volume of atrophic voxels 260.61 cm^3; Fig 2).

These results were driven by patients with WM lesions. When only patients with WM lesions were considered, the patterns of GM atrophy in both groups of MOGAD and AQP4+NMOSD patients with WM lesions when compared with HC did not change (Fig S2). Instead, when only patients without lesions were investigated, no differences in GM volumes were observed between MOGAD and AQP4+NMOSD patients and HC. Table S1 summarizes GM regions whose volume was significantly different between groups and their corresponding total volume in cm^3 and total number of voxels. The same patterns of GM atrophy were observed when disease duration and time to last attack were independently used as covariates (Table S2).

Differences in GM Volumes Between the Three Disease Groups

Patients with MOGAD showed more pronounced volume loss in the temporal cortex than RRMS (6.71 cm^3), whereas atrophy in the occipital cortex was more prominent in AQP4+NMOSD than in RRMS (19.82 cm^3). Conversely, RRMS showed more pronounced deep GM tissue loss compared with MOGAD (27.90 cm^3) and AQP4+NMOSD (47.04 cm^3). No differences were detected between MOGAD and AQP4+NMOSD (Fig 2). When only patients with WM lesions were included in the analysis, the results remained consistent in terms of distribution and were more significant (Fig S2). When considering only patients without WM lesions, differences in GM areas were more limited than when considering all patients together (Fig S3). Patients with MOGAD without brain lesions showed atrophy in the bilateral frontal cortex when compared with MOGAD with brain lesions (8.06 cm^3), whereas no differences were found between patients in the AQP4+NMOSD group (Fig 3). When disease duration and time to last attack were independently used as covariates, the same patterns of atrophy were observed (Table S2). No significant differences in atrophy patterns were found in treated versus untreated MOGAD patients.

Topographic Distribution of GM Atrophy in Relation to Lesions

In MOGAD, a higher number of cortical/juxtacortical lesions was associated with reduced volume in the subcortical regions (ie, thalamus, caudate, amygdala), bilateral insula, and hippocampus (total volume of atrophic voxels 22.65 cm^3). In addition, there was an association between a higher number of periventricular lesions and reduced volume in the insula and thalamus and in the left temporal cortex (total volume of atrophic voxels 62.16 cm^3;

Table 1. Demographic and Clinical Characteristics of Myelin Oligodendrocyte Glycoprotein Antibody Associated Disease, Aquaporin-4-Antibody-Positive Neuromyelitis Optica Spectrum Disorder, Relapsing–Remitting Multiple Sclerosis, and Healthy Controls

	MOGAD[a] (n = 135)	AQP4+NMOSD (n = 135)	RRMS (n = 175)	Healthy controls (n = 144)	p value[b]
Sex (M/F)	52/83	24/111	54/121	57/87	<0.001
Mean age at MRI, yr (SD)	40.9 (14.1)	51.1 (13.9)	39.8 (10.5)	37.2 (11.4)	<0.001
Mean age at onset, yr (SD)	34.1 (14.3)	42.9 (15.2)	32.0 (8.6)	NA	<0.001
Median disease duration, yr (range)	3.5 (0.3–47.1)	6.3 (0.4–40.7)	6.1 (0.3–29.3)	NA	0.019
Median time from last attack to MRI, mo (range)	15 (3–404)	27 (3–210)	17 (3–225)	NA	<0.001
Median EDSS at MRI (range)	2 (0–7.5)	3.5 (0–8)	2 (0–8)	NA	0.001
No. patients on treatment (%)	77 (57%)	121 (90%)	175 (100%)	NA	0.001
Phenotype at onset, n (%) patients					
Unilateral ON	39 (29)	37 (27)	35 (20)	NA	0.001
Bilateral ON	27 (20)	9 (7)	3 (2)	NA	
TM	36 (27)	45 (33)	35 (20)	NA	
ON + TM	13 (10)	10 (8)	1 (1)	NA	
ADEM	6 (4)	0	1 (1)	NA	
Others	7 (5)[c]	16 (12)	72 (41)	NA	
NA	7 (5)	18 (13)	28 (16)	NA	
Disease course, n (%) patients					
Monophasic	38 (28)	16 (12)	0	NA	0.001
Relapsing	87 (65)	100 (74)	175 (100)	NA	
NA	10 (7)	19 (14)	0	NA	
No. patients on all disease-modifying treatment (%)	75 (55)	121 (90)	175 (100)	NA	0.001
No. patients on MS disease-modifying agents[d] (%)	2 (13)	0	167 (95)	NA	
No. patients on other therapies[e] (%)	73 (54)	121 (90)	8 (5)	NA	

ADEM = acute disseminated encephalomyelitis; AQP4+NMOSD = aquaporin-4 antibody-positive neuromyelitis optica spectrum disorder; EDSS = Expanded Disability Status Scale; MRI = magnetic resonance imaging; MOGAD = myelin oligodendrocyte glycoprotein antibody-associated disease; MS = multiple sclerosis; NA = non-available, ON = optic neuritis; RRMS = relapsing–remitting multiple sclerosis; TM = transverse myelitis.

[a]Among the patients with the information available, 121/130 (93%) satisfied the international criteria for MOGAD (Banwell et al., *Lancet Neur* 2023), and 9/130 (7%) had the diagnosis confirmed by the typical clinical phenotype for MOGAD and repeated positivity in antibody testing using a cell-based assay without reported titer, but with no supporting features.

[b]Using Kruskal–Wallis, ANOVA or χ^2-test, as appropriate, depending on the nature of the variable.

[c]Six patients with brainstem involvement, 1 patient with unilateral tumefactive hemispheric lesion.

[d]MS disease-modifying agents included medications approved for MS: interferon, glatiramer acetate, teriflunomide, dimethylfumarate, cladribine, fingolimod, natalizumab, alemtuzumab, and ocrelizumab.

[e]Other therapies included: azathioprine, mycophenolate mofetil, rituximab, intravenous immunoglobulin G, cyclophosphamide, methotrexate, mitoxantrone, and satralizumab.

Table 2. Number and Volume of Lesions in Myelin Oligodendrocyte Glycoprotein Antibody Associated Disease, Aquaporin-4-Antibody-Positive Neuromyelitis Optica Spectrum Disorder, Relapsing–Remitting Multiple Sclerosis, and Healthy Controls, According to Lesion Location

	MOGAD (n = 135)	AQP4+NMOSD (n = 135)	RRMS (n = 175)	Healthy controls (n = 144)	*p* value[a]
No. patients with brain lesions (%)	92/135 (68%)	108/135 (80%)	175/175 (100%)	33/144 (23%)	<0.001
No. brain lesions, mean (SD)	6.76 (12.36)	10.16 (13.68)	27.08 (21.37)	1.01 (3.71)	<0.001
Brain lesion volume, mm^3 mean (SD)	2771.52 (8733.27)	3997.02 (10454.49)	8269.24 (8971.71)	51.73 (185.87)	<0.001
No. cortical/juxtacortical lesions, mean (SD)	2.67 (5.66)	3.47 (6.86)	8.63 (10.94)	0.32 (1.09)	<0.001
Mean volume of cortical/juxtacortical lesions, mm^3 (SD)	1356.02 (5529.86)	1340.71 (5480.95)	2154.93 (4162.93)	19.91 (73.63)	<0.001
No. periventricular lesions, mean (SD)	0.90 (1.67)	1.32 (1.86)	5.78 (4.18)	0.07 (0.28)	<0.001
Mean volume of periventricular lesions, mm^3 (SD)	1,177,63 (5124.62)	2219.19 (8040.25)	5027.64 (6742.75)	7.76 (45.11)	<0.001
No. mixed deep GM/deep WM lesions, mean (SD)	0.04 (0.24)	0.13 (0.50)	0.33 (0.73)	0 (0)	<0.001
Mean volume of mixed deep GM/deep WM lesions, mm^3 (SD)	3.09 (18.20)	8.62 (34.97)	22.47 (61.65)	0 (0)	<0.001
No. deep WM lesions, mean (SD)	2.87 (5.60)	4.93 (7.10)	11.28 (9.50)	0.61 (2.61)	<0.001
Mean volume of deep WM lesions, mm^3 (SD)	195.94 (400.11)	374.72 (626.03)	937.01 (994.78)	23.18 (94.62)	<0.001
No. infratentorial lesions, mean (SD)	0.29 (0.94)	0.31 (0.73)	1.06 (2.08)	0.01 (0.08)	<0.001
Mean volume of infratentorial lesions, mm^3 (SD)	38.84 (158.37)	53.78 (109.51)	127.19 (327.47)	0.88 (10.54)	<0.001
Mean whole brain volume, cm^3 (SD)[b]	1,480 (71.23)	1,442 (90.01)	1,478 (85.48)	1,505 (79.29)	<0.01
Mean gray matter volume, cm^3 (SD)[b]	802.16 (56.52)	775.26 (71.69)	806.56 (61.65)	823.56 (57.92)	<0.01

[a]Using ANOVA.

[b]Obtained using SIENAX2 (Luchetti et al., ECTRIMS 2019). Please note that the AQP4+NMOSD group shows here lower whole brain and gray matter volumes in comparison with the other 2 patient groups, but this should be largely attributed to the older age of patients within this cohort, and this difference disappeared when data were age-corrected.

[a]AQP4+NMOSD = aquaporin-4 antibody-positive neuromyelitis optica spectrum disorder; GM + gray matter; MS = multiple sclerosis; MOGAD = myelin oligodendrocyte glycoprotein antibody-associated disease; RRMS = relapsing–remitting multiple sclerosis; WM = white matter.

Fig 4), which persisted independently of the number of cortical/juxtacortical lesions. The results remain consistent in terms of distribution, but more significant ($p < 0.01$) when only patients with MOGAD and WM lesions were included in the analysis.

In RRMS, a higher number of cortical/juxtacortical lesions was associated with reduced volume in the deep GM and insula (total volume of atrophic voxels 9.55 cm^3); a higher number of periventricular lesions was associated with reduced volume in the bilateral deep GM, thalamus, temporal, and parietal cortex (total volume of atrophic voxels 67.59 cm^3); a higher number of deep WM lesions was associated with reduced volume in the insula, thalamus, putamen, and temporal and occipital cortex (total volume of atrophic voxels 10.46 cm^3); a higher number of infratentorial lesions was associated with reduced volume in the bilateral thalamus, left putamen, and left caudate (total volume of atrophic voxels: 6.33 cm^3; Fig 4). The association between higher number of periventricular lesions with reduced GM volume
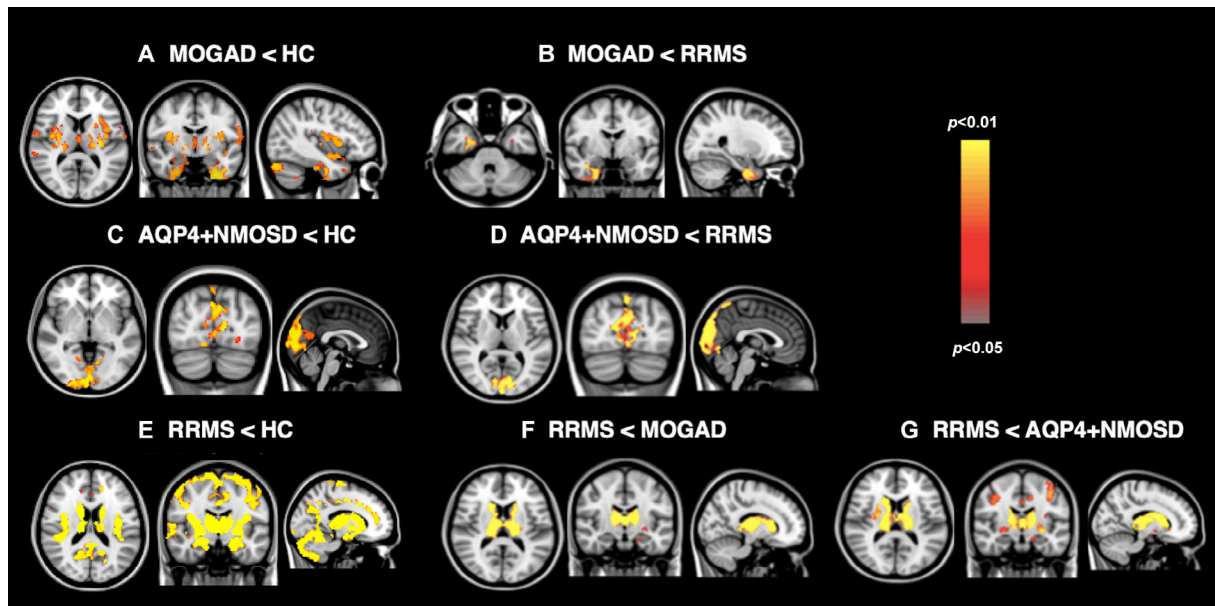
Figure 2: Differences in gray matter (GM) volumes between myelin oligodendrocyte glycoprotein antibody-associated disease (MOGAD), aquaporin-4 antibody-positive neuromyelitis optica spectrum disorder (AQP4+NMOSD), relapsing–remitting multiple sclerosis (RRMS), and healthy controls (HC) using a voxel-wise analysis. Topographical distribution of group differences in GM atrophy. Atrophied voxels are shown in a color scale from yellow to red, from the most to the least significant, respectively. Regions with lower GM volume in MOGAD compared with (A) HC and (B) RRMS; regions with lower GM atrophy in AQP4 +NMOSD compared with (C) HC and (D) RRMS; regions with lower GM atrophy in RRMS compared with (E) HC, (F) MOGAD, and (G) AQP4 + NMOSD. No differences were detected between MOGAD and AQP4+NMOSD. [Color figure can be viewed at www.annalsofneurology.org]
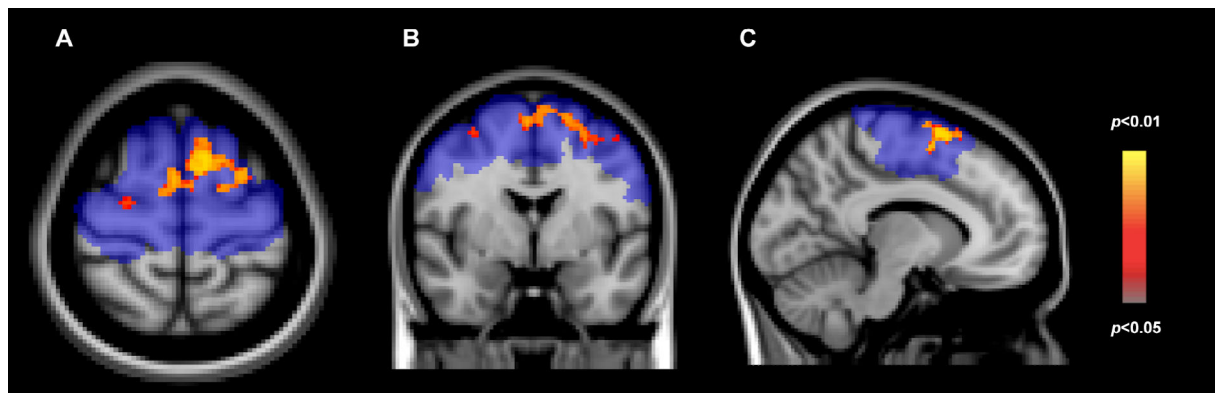

Figure 3: Differences in gray matter (GM) volumes between myelin oligodendrocyte glycoprotein antibody-associated disease (MOGAD) with and without brain lesions using a voxel-wise analysis. Topographical distribution of group differences in GM atrophy. Atrophied voxels are shown in a color scale from yellow to red, from the most to the least significant, respectively, in the (A) axial, (B) coronal, and (C) sagittal planes. The Julich brain atlas of the FSL tool was used to localize the atrophic voxels within the cortex. In MOGAD patients without brain lesions compared with those with at least one brain lesion, regions with lower GM volume were identified. The overlaid atlas revealed that the atrophic voxels were situated in the motor cortex, shown in blue.[35] [Color figure can be viewed at www.annalsofneurology.org]

persisted independently of the number of lesions on other locations.

In AQP4+NMOSD, there was no association between lesion distribution and GM atrophy, both when keeping all patients together (those with lesions and those without lesions) and when considering patients with lesions only.

When considering total T2 lesion volume, we found that in MOGAD, a higher T2 lesion volume was associated to a higher degree of atrophy in the deep GM, insula, and temporal cortex (total volume of atrophic voxels 74.57 cm^3). Similarly, in RRMS, a higher T2 lesion volume was associated with an increased degree of atrophy in the deep GM and insula (total volume of atrophic voxels
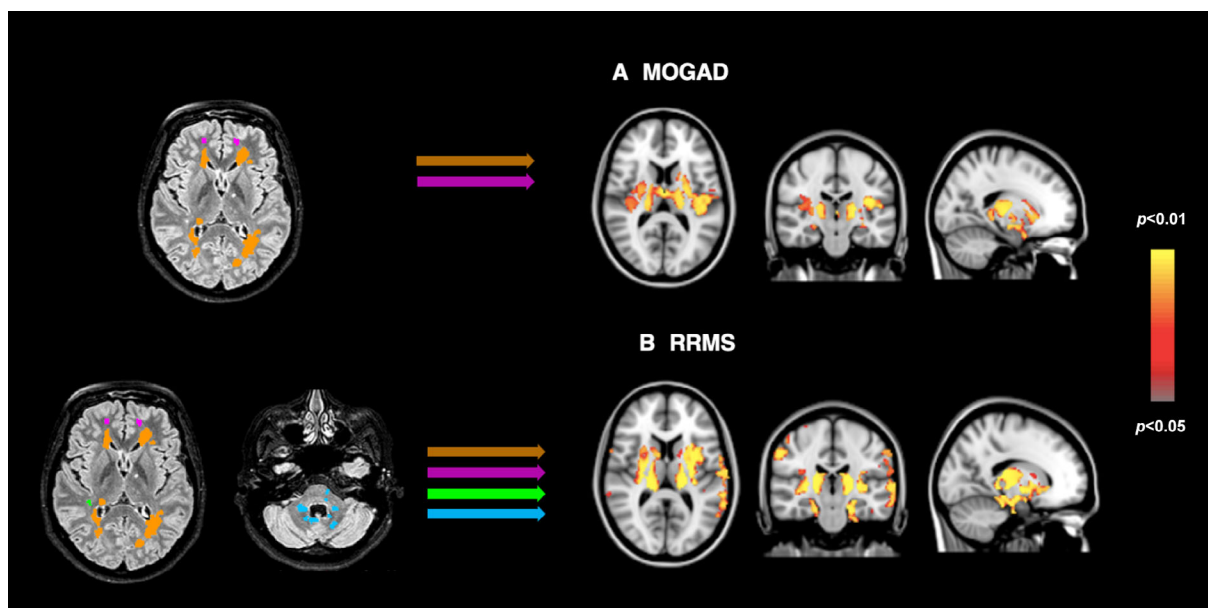
Figure 4: Association between lesion distribution and gray matter (GM) volumes reduction in myelin oligodendrocyte glycoprotein antibody-associated disease (MOGAD) and relapsing remitting multiple sclerosis (RRMS). Lesions distribution significantly associated with reduced GM volumes. Lesions are shown in different colors according to their locations, respectively, cortical/juxtacortical (pink), periventricular (orange), deep white matter (green), and infratentorial (light blue); atrophied voxels are shown in a color scale from yellow to red, from the most to the least significant, respectively. (A) In MOGAD, a higher number of periventricular and cortical/juxtacortical lesions were associated with reduced volume in the temporal cortex, deep GM, and insula. (B) In RRMS, a higher number of cortical/juxtacortical, periventricular, deep white matter, and infratentorial lesions were associated with reduced volume in the frontal, parietal, temporal cortex, deep GM, and insula. No correlation was found between lesions and GM volumes in aquaporin-4 antibody-positive neuromyelitis optica spectrum disorder. [Color figure can be viewed at www.annalsofneurology.org]

32.70 cm^3). By contrast, no such association was observed in AQP4+NMOSD.

Topographic Distribution of GM Atrophy in Relation to History of Optic Neuritis and Transverse Myelitis

In AQP4+NMOSD, patients with history of ON and TM ($n = 49$) showed a higher degree of GM atrophy than those with history of ON only ($n = 30$; ie, bilateral insula, occipital and temporal cortex, cerebellum; 111.36 cm^3) and those with history of TM only ($n = 43$; ie, right insula, right temporal cortex, bilateral occipital cortex, cerebellum; total volume of atrophic voxels 48.58 cm^3). By contrast, ON and TM patients did not show differences in GM atrophy. Finally, there were not differences in GM atrophy between the three groups of MOGAD patients (ON, $n = 49$; TM, $n = 33$; ON + TM, $n = 49$).

Discussion

In this extensive, multicenter study, we observed distinct patterns and degrees of GM atrophy in individuals with RRMS, MOGAD, and AQP4+NMOSD. Specifically, we found that: (1) in RRMS, as expected, there was widespread GM atrophy, with a pronounced involvement of the deep GM; (2) in MOGAD, GM atrophy was less diffuse, primarily affecting the temporal cortex, and (3) in AQP4+NMOSD, GM atrophy was limited to the occipital cortex. Additionally, the present study revealed a correlation between regional atrophy and the distribution of lesions in MOGAD, suggesting that, similar to RRMS, focal WM damage plays a role in GM pathology.

The development of GM atrophy is generally attributed to progressive neuronal damage.[25] In both MOGAD and RRMS, we observed GM damage in cortical and subcortical regions, indicating the involvement of common neurodegenerative pathways in tissue injury for both disorders. Neuropathological studies in MOGAD revealed widespread cortical demyelination, which may contribute to atrophy development. Similar to MS, cortical demyelination in MOGAD is associated with meningeal inflammation, suggesting a link between meningeal inflammatory processes and GM damage.[8,26] As prolonged exposure to static inflammatory cytokines in the temporal area has been demonstrated to be associated with the increased occurrence of neurodegeneration in MS,[27] the compartmentalized inflammation in the meninges might be a major driver of the GM damage seen in our MOGAD group. In our study, this occurred specifically in the insular and temporal cortex, perhaps due to the dynamic

restrictions that the cerebrospinal fluid flow may encounter within the cerebral sulci and deep cortex invaginations occurring in these regions.[28] Interestingly, our findings also demonstrated that GM atrophy is overall less severe and diffuse in MOGAD than in RRMS. This aligns with a recent MRI study using a sensitive quantitative technique (ie, T2 relaxation times), showing that, although abnormal, non-lesional GM in MOGAD shows fewer microstructural changes than in MS.[29] The difference in the extent of the damage may reflect more efficient recovery in MOGAD, and this could impact the distinct disease course of these conditions.[8]

An additional mechanism contributing to GM atrophy in MS is retrograde neurodegeneration of WM tracts transected by lesions.[30] The present study revealed that reduced GM volumes in MOGAD, specifically in the temporal cortex, deep GM, and insula, were driven by patients with WM lesions. Specifically, lower GM volumes of atrophic areas were associated with a higher number of periventricular and cortical/juxtacortical lesions, and this association persisted even when the analysis was restricted to patients with WM lesions. The temporal cortex maintains connections through association fibers to all forebrain lobes.[31] Likewise, the deep GM, especially the thalamus, shows extensive projections to the cerebral cortex. Additionally, the insula features an intricate network of connections with both cortical and subcortical structures.[32] This suggests that disruption of these extensive connections due to WM lesions may lead to retrograde neurodegeneration, culminating in GM atrophy in these regions.[33] Our results show that global lesion load is also important to contribute to GM atrophy, which therefore also reflects global WM tissue damage. Future investigations, using probabilistic methods and microstructural tissue-sensitive techniques, can deepen our understanding of trans-synaptic degeneration in MOGAD. Notably, our findings along the ventricular surface indicate an association between lesions and atrophy, independent of other lesion locations. Recent research suggests MOG immunoglobulin G production in the CNS may be more common than AQP4 immunoglobulin G, indicating differing B-cell trafficking and antibody production in MOGAD and AQP4 +NMOSD.[34] This may explain varied tissue injury near the cerebrospinal fluid in these diseases. Further research is needed for clarity.

Interestingly, we observed that patients with MOGAD without brain lesions showed more damage in the frontal cortex compared with those with brain lesions, whereas we found no differences between patients with history of ON only and TM only. These findings further emphasize the impact of WM lesions on GM atrophy

development, and highlight the intricate interactions among different regions within the CNS in the context of MOGAD pathology. We can speculate that in patients with isolated cord involvement, cord lesions may sever the corticospinal tracts projecting to the motor area situated in the frontal cortex, a region where we identified atrophic voxels in our study.[35] Conversely, in patients with concurrent brain and cord involvement, the damage to the frontal cortex may be concealed by the presence of WM lesions, making it challenging to isolate the distinct contributions of each compartment to GM atrophy. Further investigations should encompass other cord segments, such as the thoracolumbar and conus regions, which are preferentially affected in MOGAD, to accurately assess the interplay between brain and cord damage in this disease.

Although both MOGAD and RRMS show GM atrophy, clinical distinctions arise due to the absence of a progressive disease course in MOGAD. In this respect, several interpretations can be considered. First, in MOGAD, up to 78% of brain lesions may resolve during remission, making it challenging to assess lesion-related atrophy.[10,36] For instance, the present study did not find a link between reduced cerebellar atrophy in MOGAD and lesions. It is plausible that cerebellar involvement results from direct MOG antibody-mediated inflammation, as fluffy infratentorial lesions are distinctive features of the acute phase that may have resolved over time.[9] Second, changes in brain volume in MOGAD might be reversible and reflect symptom resolution, influenced by various factors, such as anti-inflammatory treatments and inflammatory cell volume changes.[37,38] Finally, the occurrence of brain atrophy without clinical progression in MOGAD mirrors the optic neuritis paradox, where functional improvements occur despite residual retinal damage.[39] MOGAD's evolving nature calls for further follow-up studies to explore the potential reversibility and long-term effects of atrophy on the clinical course.

In contrast to MOGAD and RRMS, the present study revealed more localized changes in the AQP4 +NMOSD group, specifically in the occipital cortex. This differs from earlier studies that did not report differences in occipital cortex volume.[40,41] However, previous works did reveal optic pathway damage in AQP4+NMOSD. This was shown as reduced fractional anisotropy and increased functional connectivity in the primary visual network, linked to impaired vision and potentially associated with atrophy.[13,41,42] It is likely that the larger sample size of our study enabled the detection of changes that prior studies with smaller cohorts might have overlooked. Notably, the selective involvement of the occipital cortex

in AQP4+NMOSD aligns with the disease's known connection to optic neuritis and visual pathway involvement.[43]

In AQP4+NMOSD, unlike MOGAD and RRMS, cortical demyelination and meningeal infiltrates are not observed.[25,44] Therefore, other mechanisms are likely responsible for cortical involvement in this disease. NMOSD relapses often affect the visual system, particularly with optic neuritis as a common initial symptom in our cohort. These relapses can be severe and lead to incomplete recovery. Based on this, it can be hypothesized that the involvement of the occipital lobes is associated with the trans-synaptic damage through the optic radiation due to the optic nerve lesions.[45] The typical posterior location of the optic nerve lesions, along with the significant damage observed in the optic pathways on tract-based analyses, support our hypothesis.[13,41] Similar findings have been observed in glaucoma patients with visual impairment, where chronic reduction of visual input was associated with changes in WM tracts and decreased connectivity in visual networks, leading to atrophy of the visual cortex.[46] Further research is needed to explore the functional implications of these occipital cortex changes in AQP4+NMOSD, and their relationship to visual symptoms and disability in affected individuals.

In the present study involving a large cohort of AQP4+NMOSD patients, we found no correlation between brain lesions and GM volumes, distinguishing it from MOGAD and RRMS. AQP4+NMOSD lesions show diverse patterns, with some causing extensive axonal damage and secondary Wallerian tract degeneration, whereas others selectively affect astrocytes without demyelination or neurodegeneration.[47] These brain lesions in AQP4+NMOSD tend to localize near high AQP4 expression regions, possibly involving selective pathways and fewer tracts.[48] Therefore, it is plausible that periventricular lesions characteristic of MS may cause more direct GM atrophy through Wallerian degeneration than brainstem lesions typical of NMOSD, potentially explaining the lack of correlation between WM lesion location and GM atrophy in NMOSD. Additionally, it is worth noting that our AQP4+NMOSD patients were older than those in the other two groups, which raises the possibility of age-related vascular damage contributing to some of these lesions, although this remains inconclusive. Finally, the present results indicated that in AQP4+NMOSD, when both the optic nerve and spinal cord are affected, patients show greater GM atrophy compared with cases where these compartments are involved in isolation. This underscores the significance of WM focal damage in atrophy development, particularly when the damage is extensive and affects multiple systems.

The present study had certain limitations. First, the recruitment of patients was conducted before the international criteria for MOGAD diagnosis were established.[5] However, in line with the literature,[49] the majority of patients satisfied the criteria, and in the others, the diagnosis was made in specialized centers, based on typical clinical history and clear MOG antibody positivity.[19] Second, due to the unavailability of dedicated MRI scans, we could not include optic nerve and spinal cord lesions in our analysis. It would be valuable for future research to investigate whether the involvement of other CNS compartments, beyond the brain, may impact the GM damage. Third, the analysis conducted on subgroups of patients might be subject to a reduction in statistical power. Consequently, any interpretations or speculations derived from these subgroup analyses should be approached with caution. Moreover, the cross-sectional design of our study prevented the assessment of changes over time, which are crucial in understanding the progression of chronic diseases. Finally, the timing of the MRI scan was several years after disease diagnosis, and this leads to the consideration that these results can be extrapolated only to patients with well-established disease. Future longitudinal MRI studies are warranted to examine whether the baseline distribution of lesions could influence the development of atrophy throughout the disease course and to elucidate the temporal evolution of atrophy, particularly in the context of MOGAD.

In conclusion, the present study highlights similarities and differences in GM damage between MOGAD, RRMS, and AQP4+NMOSD. Both MOGAD and RRMS show GM damage in regions close to the cerebrospinal fluid, and show associations between higher WM lesion burden and reduced GM volume. However, the mechanisms of repair in MOGAD may limit the extent of damage compared with RRMS. Conversely, in AQP4+NMOSD, the selective occipital cortical involvement may be a secondary consequence of optic pathway disruption, whereas WM lesions do not seem to be implicated in the observed neurodegenerative processes in this disease. These findings contribute to a better understanding of the distinct pathogenic mechanisms underlying tissue damage in these neurological disorders. Further research is needed to investigate the long-term implications of GM damage and the role of other CNS compartments in these diseases, and may focus on replicating these findings within new cohorts to assess the discriminatory capability of individual-level atrophy measures. This would pave the way for using atrophy metrics as biomarkers for disease diagnosis.

Author Contributions

R.C., O.C., and N.D.S. contributed to the conception and design of the study. M.B., F.P., G.G., L.L., A.B., L.H., A.J., J.P., S.M., F.P., R.M., F.D.D., C.d.M.R., S.L.A.P., D.K.S, M.F., M.A.R., L.C., A.R., J.S.G., G.A., Y.L., Y.D., C.G., C.T., S.R., M.P.A., M.U., S.G., M.G., S.L., M.S., C.L., B.B., R.S., P.S., E.G.C., A.K.P., C.G., Ö.Y., J.M., B.S., B.B., and F.B. contributed to the acquisition and analysis of data. R.C., O.C., and NDS contributed to drafting the text or preparing the figures.

Potential Conflicts of Interest

Data Availability

Anonymized data not published within this article will be made available by request from any qualified investigator.

Authors are members of the MAGNIMS network (Magnetic Resonance Imaging in MS; https://www.magnims.eu/), which is a group of European clinicians and scientists with an interest in undertaking collaborative studies using MRI methods in multiple sclerosis, independent of any other organization and is run by a steering committee whose members are: F. Barkhof, N. de Stefano, J. Sastre-Garriga, O. Ciccarelli, C. Enzinger, M. Filippi, C. Gasperini, L. Kappos, J. Palace, H. Vrenken, À. Rovira, M.A. Rocca and T. Yousry.

References

1. Lassmann H. The changing concepts in the neuropathology of acquired demyelinating central nervous system disorders. Curr Opin Neurol 2019;32:313–319. https://doi.org/10.1097/wco.0000000000000685.

2. Marignier R, Hacohen Y, Cobo-Calvo A, et al. Myelin-oligodendrocyte glycoprotein antibody-associated disease. Lancet Neurol 2021;20:762–772. https://doi.org/10.1016/S1474-4422(21)00218-0.

3. Kuhlmann T, Marcello M, Timothy C, et al. "Personal View Multiple Sclerosis Progression: Time for a New Mechanism-Driven Framework." The Lancet Global Health 2022. https://doi.org/10.1016/S1474-4422(22)00289-7.

4. Ciccarelli O, Cohen JA, Reingold SC, et al. Spinal cord involvement in multiple sclerosis and neuromyelitis optica spectrum disorders. Lancet Neurol 2019;18:185–197. https://doi.org/10.1016/S1474-4422(18)30460-5.

5. Banwell B, Bennett JL, Marignier R, et al. Diagnosis of myelin oligodendrocyte glycoprotein antibody-associated disease: international MOGAD panel proposed criteria. Lancet Neurol 2023;4422:1–15. https://doi.org/10.1016/s1474-4422(22)00431-8.

6. Frischer JM, Bramow S, Dal-Bianco A, et al. The relation between inflammation and neurodegeneration in multiple sclerosis brains. Brain 2009;132:1175–1189. https://doi.org/10.1093/brain/awp070.

7. Takai Y, Misu T, Suzuki H, et al. Staging of astrocytopathy and complement activation in neuromyelitis optica spectrum disorders. Brain 2021;144:2401–2415. https://doi.org/10.1093/BRAIN/AWAB102.

8. Höftberger R, Guo Y, Flanagan EP, et al. The pathology of central nervous system inflammatory demyelinating disease accompanying myelin oligodendrocyte glycoprotein autoantibody. Acta Neuropathol 2020;139:875–892. https://doi.org/10.1007/s00401-020-02132-y.

9. Juryńczyk M, Tackley G, Kong Y. Brain lesion distribution criteria distinguish MS from AQP4-antibody NMOSD and MOG-antibody disease. J Neurol Neurosurg Psychiatry 2017;88:132–136. https://doi.org/10.1136/jnnp-2016-314005.

10. Sechi E, Krecke KN, Messina SA, et al. Comparison of MRI lesion evolution in different central nervous system demyelinating disorders. Neurology 2021;97:e1097–e1109. https://doi.org/10.1212/WNL.0000000000012467.

11. Cortese R, Carrasco FP, Tur C, et al. Differentiating multiple sclerosis from AQP4-Neuromyelitis Optica Spectrum disorder and MOG-antibody disease with imaging. Neurology 2022;100:e308-e323. https://doi.org/10.1212/WNL.0000000000201465.

12. Duan Y, Zhuo Z, Li H, et al. Brain structural alterations in MOG antibody diseases: a comparative study with AQP4 seropositive NMOSD and MS. J Neurol Neurosurg Psychiatry 2021;92:709–716. https://doi.org/10.1136/jnnp-2020-324826.

13. Messina S, Mariano R, Roca-Fernandez A, et al. Contrasting the brain imaging features of MOG-antibody disease, with AQP4-antibody NMOSD and multiple sclerosis. 2021;28:217–227. https://doi.org/10.1177/13524585211018987.

14. Lotan I, Billiet T, Ribbens A, et al. Volumetric brain changes in MOGAD: a cross-sectional and longitudinal comparative analysis. Mult Scler Relat Disord 2023;69:69. https://doi.org/10.1016/j.msard.2022.104436.

15. Duan Y, Liu Y, Liang P, et al. Comparison of grey matter atrophy between patients with neuromyelitis optica and multiple sclerosis: a voxel-based morphometry study. Eur J Radiol 2012;81:e110–e114. https://doi.org/10.1016/j.ejrad.2011.01.065.

16. Jehna M, Pirpamer L, Khalil M, et al. Periventricular lesions correlate with cortical thinning in multiple sclerosis. Ann Neurol 2015;78:530–539. https://doi.org/10.1002/ANA.24461.

17. Bodini B, Veronese M, García-Lorenzo D, et al. Dynamic imaging of individual Remyelination profiles in multiple sclerosis. Ann Neurol 2016;79:726–738. https://doi.org/10.1002/ana.24620.

18. Zhang J, Giorgio A, Vinciguerra C, et al. Gray matter atrophy cannot be fully explained by white matter damage in patients with MS. Mult Scler J 2020;27:39–51. https://doi.org/10.1177/1352458519900972.

19. Cortese R, Battaglini M, Prados F, et al. Clinical and MRI measures to identify non-acute MOG-antibody disease in adults. Brain 2022;14:2489–2501. https://doi.org/10.1093/BRAIN/AWAC480.

20. Wingerchuk DM, Banwell B, Bennett JL, et al. International consensus diagnostic criteria for neuromyelitis optica spectrum disorders. Neurology 2015;85:177–189. https://doi.org/10.1212/WNL.0000000000001729.

21. Thompson AJ, Banwell BL, Barkhof F, et al. Diagnosis of multiple sclerosis: 2017 revisions of the McDonald criteria. Lancet Neurol 2018;17:162–173. https://doi.org/10.1016/S1474-4422(17)30470-2.

22. LST–Lesion segmentation for SPM. Paul Schmidt–freelance statistician, Accessed July 19, 2021. https://www.applied-statistics.de/lst.html.

23. Filippi M, Preziosa P, Banwell BL, et al. Assessment of lesions on magnetic resonance imaging in multiple sclerosis: practical guidelinesfile. Brain 2019;142:1858–1875. https://doi.org/10.1093/brain/awz144.

24. Nichols TE, Holmes AP. Nonparametric permutation tests for functional neuroimaging: a primer with examples. Hum Brain Mapp 2002;15:1–25. https://doi.org/10.1002/HBM.1058.

25. Kawachi I, Lassmann H. Neurodegeneration in multiple sclerosis and neuromyelitis optica. J Neurol Neurosurg Psychiatry 2017;88:137–145. https://doi.org/10.1136/JNNP-2016-313300.

26. Elsbernd P, Cacciaguerra L, Krecke KN, et al. Cerebral enhancement in MOG antibody-associated disease. J Neurol Neurosurg Psychiatry 2023;95:14–18. https://doi.org/10.1136/JNNP-2023-331137.

27. Mahad DH, Trapp BD, Lassmann H. Pathological mechanisms in progressive multiple sclerosis. Lancet Neurol 2015;14:183–193. https://doi.org/10.1016/S1474-4422(14)70256-X.

28. Abbott NJ. Evidence for bulk flow of brain interstitial fluid: significance for physiology and pathology. Neurochem Int 2004;45:545–552. https://doi.org/10.1016/J.NEUINT.2003.11.006.

29. Brier MR, Xiang B, Ciotti JR, et al. Quantitative MRI identifies lesional and non-lesional abnormalities in MOGAD. Mult Scler Relat Disord 2023;73:104659. https://doi.org/10.1016/J.MSARD.2023.104659.

30. Haider L, Zrzavy T, Hametner S, et al. The topograpy of demyelination and neurodegeneration in the multiple sclerosis brain. Brain 2016;139:807–815. https://doi.org/10.1093/brain/awv398.

31. Kiernan JA. Anatomy of the temporal lobe. Epilepsy Res Treat 2012;2012:1–12. https://doi.org/10.1155/2012/176157.

32. Ghaziri J, Tucholka A, Girard G, et al. Subcortical structural connectivity of insular subregions. Sci Rep 2018;8:1–12. https://doi.org/10.1038/s41598-018-26995-0.

33. Calabrese M, Magliozzi R, Ciccarelli O, et al. Exploring the origins of grey matter damage in multiple sclerosis. Nat Rev Neurosci 2015;16:147–158. https://doi.org/10.1038/nrn3900.

34. Akaishi T, Takahashi T, Misu T, et al. Difference in the source of anti-AQP4-IgG and anti-MOG-IgG antibodies in CSF in patients with Neuromyelitis Optica Spectrum disorder. Neurology 2021;97:e1–e12. https://doi.org/10.1212/WNL.0000000000012175.

35. Geyer S. The microstructural border between the motor and the cognitive domain in the human cerebral cortex. Adv Anat Embryol Cell Biol 2004;174:174. https://doi.org/10.1007/978-3-642-18910-4.

36. Cacciaguerra L, Redenbaugh V, Chen JJ, et al. Timing and predictors of T2-lesion resolution in patients with myelin-oligodendrocyte-glycoprotein-antibody-associated disease. Neurology 2023;101:e1376–e1381. https://doi.org/10.1212/WNL.0000000000207478.

37. Shan D, Li S, Xu R, et al. Post-COVID-19 human memory impairment: a PRISMA-based systematic review of evidence from brain imaging studies. Front Aging Neurosci 2022;14:14. https://doi.org/10.3389/fnagi.2022.1077384.

38. Cortese R, Battaglini M, Sormani MP, et al. Reduction in grey matter atrophy in patients with relapsing multiple sclerosis following treatment with cladribine tablets. Eur J Neurol 2022;11:179–186. https://doi.org/10.1111/ENE.15579.

39. Sotirchos ES, Filippatou A, Fitzgerald KC, et al. Aquaporin-4 IgG seropositivity is associated with worse visual outcomes after optic neuritis than MOG-IgG seropositivity and multiple sclerosis, independent of macular ganglion cell layer thinning. Mult Scler 2019;26:1352458519864928–1352458519861371. https://doi.org/10.1177/1352458519864928.

40. Blanc F, Noblet V, Jung B, et al. White matter atrophy and cognitive dysfunctions in Neuromyelitis Optica. PLoS ONE 2012;7:e33878. https://doi.org/10.1371/journal.pone.0033878.

41. Matthews L, Kolind S, Brazier A, et al. Imaging surrogates of disease activity in Neuromyelitis Optica allow distinction from multiple sclerosis. PLoS ONE 2015;10:e0137715. https://doi.org/10.1371/journal.pone.0137715.

42. Finke C, Zimmermann H, Pache F, et al. Association of Visual Impairment in Neuromyelitis Optica Spectrum disorder with visual network reorganization. JAMA Neurol 2018;75:296–303. https://doi.org/10.1001/JAMANEUROL.2017.3890.

43. Pache F, Zimmermann H, Finke C, et al. Brain parenchymal damage in neuromyelitis optica spectrum disorder–a multimodal MRI study. Eur Radiol 2016;26:4413–4422. https://doi.org/10.1007/S00330-016-4282-X/FIGURES/3.

44. Popescu BFG, Parisi JE, Cabrera-Gómez JA, et al. Absence of cortical demyelination in neuromyelitis optica. Neurology 2010;75:2103–2109. https://doi.org/10.1212/WNL.0B013E318200D80C.

45. Tur C, Goodkin O, Altmann DR, et al. Longitudinal evidence for anterograde trans-synaptic degeneration after optic neuritis. Brain 2016;139:816–828. https://doi.org/10.1093/BRAIN/AWV396.

46. Frezzotti P, Giorgio A, Motolese I, et al. Structural and Functional Brain Changes beyond Visual System in Patients with Advanced Glaucoma. PLoS ONE 2014;9:e105931.

47. Misu T, Höftberger R, Fujihara K, et al. Presence of six different lesion types suggests diverse mechanisms of tissue injury in neuromyelitis optica. Acta Neuropathol 2013;125:815–827. https://doi.org/10.1007/s00401-013-1116-7.

48. Kim HJ, Paul F, Lana-Peixoto MA, et al. MRI characteristics of neuromyelitis optica spectrum disorder: an international update. Neurology 2015;84:1165–1173. https://doi.org/10.1212/WNL.0000000000001367.

49. Kim KH, Kim SH, Park NY, et al. Validation of the international MOGAD panel proposed criteria. Mult Scler 2023;29:1680–1683. https://doi.org/10.1177/13524585231198754.

50. Andersson JLR, Jenkinson M, Smith S. Non-linear registration aka Spatial normalisation FMRIB Technial Report TR07JA2, 2007.